Open access

https://jrisetgeotam.brin.go.id/index.php/jrisgeotam

RISET
Geologi dan Pertambangan
Geology and Mining Research

Riset Geologi dan Pertambangan (2024) Vol.34, No.2, 111–129, DOI: 10.55981/risetgeotam.2024.1343

Research article

Facies analysis and sedimentation mechanism of volcaniclastics of Cikarang Member of Jampang Formation in West Java

Naufal Anhaer[1], Moch. Indra Novian[1], Dian Novita[2]

[1] Department of Geological Engineering, Faculty of Engineering, Gadjah Mada University, Indonesia
[2] Center for Geological Survey (PSG), Geological Agency (Badan Geologi), Indonesia

Keywords:
lithofacies
depositional environment
sedimentation mechanism
gravity-flow deposition

Corresponding author:
Naufal Anhaer
Email address: anhaernaufal@gmail.com

Article history
Received : 13 November 2024
Revised : 04 December 2024
Accepted : 12 December 2024

ABSTRACT

The Cikarang Member of Jampang Formation is one of basin fills of the Bogor Basin that is characterized by gravity flow deposits. The variations of lithologies with an abundance of volcaniclastics are found in the Tonjong River in Bojongkalong Village and indicate differences in facies and sedimentation mechanisms. We measured stratigraphy of the rock units supported by petrographic analysis and paleontological analysis. The rock units consist of 11 lithofacies: graded gravel (g1G), massive gravel (m1G), massive gravelly sand (mGyS), plane-stratified laminated sand-mud couplets (slSM), massive gravel-sand couplets (mGS), plane-stratified laminated to graded mud-sand couplets (slgMS), massive sand (mS), plane-stratified gravel-sand couplets (sGS), plane-stratified laminated muddy interval sand-mud couplets (sleSM), plane-stratified laminated muddy interval mud-sand couplets (sleMS), and slump and slide deposits gravel (sdG). The depositional environment of the Cikarang Member is inner-middle fan with changes in depositional sub-environment variations in the form of channels, sandy lobes, silty-sandy distal lobes, and proximal levees with constant paleobathymetry in the lower-middle bathymetry. The volcaniclastics of the Cikarang Member of Jampang Formation is deposited in a turbid mechanism due to a turbulent current with various cohesive debris flows (mudflows) and turbidity currents scattered in each facies association.

INTRODUCTION

Sedimentary rocks cover approximately 75% of Earth's surface, with distinctive characteristics shown through texture, structure, composition, and fossil content (Boggs, 2009). These characteristics can interpret specific geological phenomena, including environmental evolution and past life events (Boggs, 2009). Java Island has unique stratigraphic features compared to Sumatra, with its central basin generally filled with gravity flow deposits (Martodjojo, 2003). The Bogor Basin in West Java shows well-exposed lithology due to less Quaternary volcanic covers (Martodjojo, 2003). The Jampang Formation, characterized by gravity flow deposits, consists of andesitic and dacitic rock fragments forming volcanic breccia, with diorite, andesite, and dacite intrusions (Van Bemmelen, 1949 in Muljana, 2023) represents the lower Miocene volcaniclastics deposited through gravity flow systems (Martodjojo, 2003).

Previous studies on the Jampang Formation in the Bogor Trough include research on tectonism and magmatism (Muljana, 2023), volcanic breccia and coarse tuff petrology (Verdiana et al., 2014), and geological study of Langkaplancar area (Hidayat et al., 2021). Martodjojo (2003, and references therein) described its depositional environment as a gravity flow system in a deep marine fan environment. The formation comprises two members: the Tuff and Breccia Member and the Cikarang Member (Effendi et al., 1998). While the Cikarang Member has been studied for nannofossil dating (Pratiwi et al., 2022), Ciomas geological site (Intan and Manurung, 2022), and geological study of Gunungbatu area (Khodijah et al., 2023). Furthermore, detailed field mapping and observation of centimeter-scale lithofacies has revealed the architectural elements of the upper Miocene deepwater submarine fan sediments has been conducted in the eastern part of Bogor Trough (Mukti et al., 2009; Mukti and Ito, 2010), and discussed its relationship with development of a transtensional basin (Armandita et al., 2009). Hence, detailed research of volcanic and carbonate-rich variations of the gravity-flow deposits in the Bogor Trough remains limited. The Tonjong River in Sukabumi reveals previously unstudied volcanic and carbonate lithologic variations (Figure 1), suggesting potential differences in facies, depositional environments, and sedimentation mechanisms. This paper reports the investigation of these aspects to better understand the evolution of the Bogor Basin.

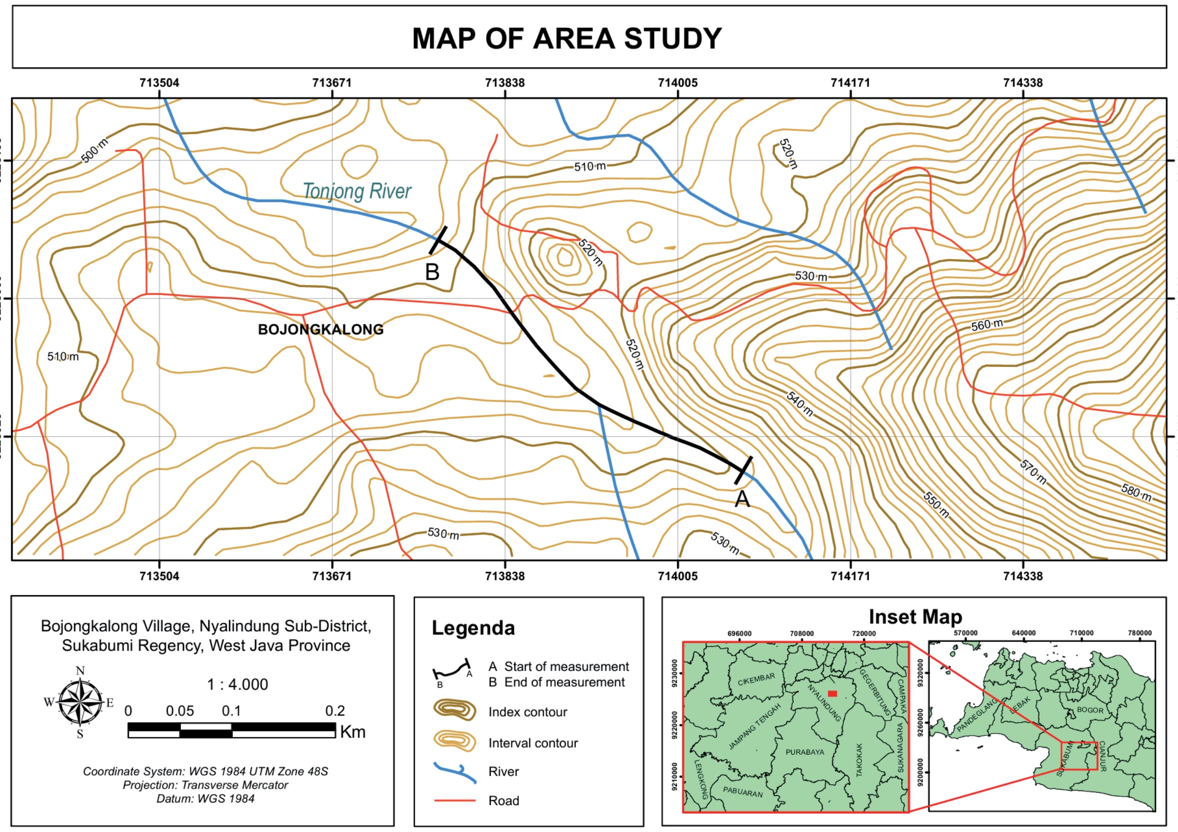

Figure 1. Research area map and topographic of study area.

STUDY AREA

The study area is included in the Regional Geological Map of the Bogor Sheet, Java, Scale 1:100,000 (Effendi et al., 1998), which is composed of the Cikarang Member of the Jampang Formation (Figure 2). The Jampang Formation is composed of massive flow breccia with a pyroxene andesite composition, dating back to the Early Miocene (Effendi et al., 1998). Van Bemmelen (1949) stated that the Jampang Formation is dominated by andesite and dacite rock fragments forming volcanic breccia, which are intruded by diorite, andesite, and dacite in some areas. Martodjojo (2003, and references therein) interpreted the Jampang Formation is deposited in a deep-sea fan depositional environment through a gravity flow system, with a thickness of up to 1235 meters.

According to Effendi et al. (1998), the Jampang Formation is composed of two members: the Cikarang Member and the Tuff and Breccia Member. The Cikarang Member is generally composed of sandy claystone interbedded with tuffaceous sandstone and tuff, with thin breccia layers (Effendi et al., 1998). Sukamto (1975) stated that the Cikarang Member is composed of tuff, lapilli tuff, tuffaceous sandstone, and clayey sandstone, deposited at depths of 500-1500 m below sea level. Martodjojo mentioned this member is composed of a sedimentary sequence of breccia, followed by massive greywacke, and towards the upper part, it becomes finer-grained and well-bedded, grading upwards into thin-bedded to laminated fine sandstone and siltstone. This member is of Early Miocene age and has an interfingering relationship with the Jampang Formation, conformably overlying the Tuff and Breccia Member of the Jampang Formation (Effendi et al., 1998).

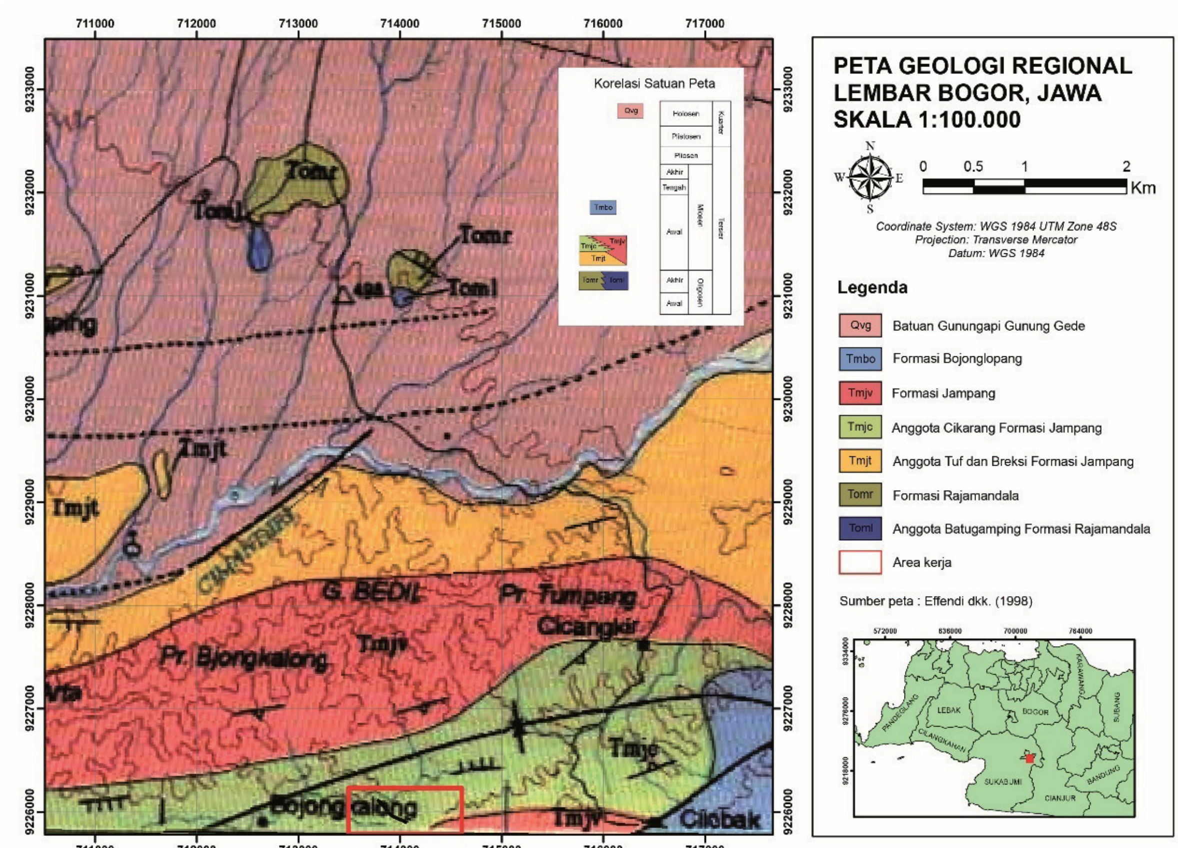

Figure 2. Regional geological map.

METHODS

Primary data were collected directly by the researcher for further analysis consists of lithology data, measured stratigraphic data, rock thin section samples, and rock sieve samples. Secondary data compiled by previous researchers and used as additional research references includes: the 1:25,000 scale Topographic Map of Indonesia, Sukabumi Regency, the 1:100,000 scale regional geological map of the Bogor Sheet, Java by Effendi et al. (1998), the 1:50,000 scale remote sensing geological map of the Sukabumi Sheet (1209-12), Java by Novita et al. (2016), and the detailed stratigraphic column of the geological mapping survey of the Sukabumi Sheet at 1:50,000 scale (Center for Geological Survey, 2016).

The data collection stage includes two sources: primary data collected directly in the field and secondary data from previous research. The secondary data was then analyzed according to the research topic. The collection of primary data focused on three main aspects: Stratigraphic observation was carried out by measuring the strike and dip of rock layers using a geological compass and recording the thickness of each layer using a Jacob's staff. This data was used to determine the vertical sequence of rock layers.

Lithological observation involved directly examining the physical properties of the rocks with the naked eye and a hand lens, checking the rock texture (color, grain size, sorting, and inter-grain relationships), and identifying sedimentary structures and carbonate content. Rock sampling was conducted for petrographic analysis (8 samples) and paleontological analysis (11 samples). The samples were used to determine lithofacies, rock age, and depositional environment.

Data processing was carried out through two main processes: laboratory analysis and measured stratigraphic analysis. For laboratory analysis, there were two types of testing: petrographic and paleontological analysis. Petrographic analysis used thin sections of rocks observed under a polarizing microscope. Rock classification followed Streckeisen (1976) for igneous rocks, Pettijohn (1987) for siliciclastic sedimentary rocks, and Mount (1985) for mixed siliciclastic-carbonate sedimentary rocks. Paleontological analysis began with crushing the rock, soaking in H2O2, sieving, and drying, then observing under a binocular microscope to identify fossils. The analysis results were used to determine the age and depositional environment.

The measured stratigraphic analysis was carried out by integrating data on strike, dip, texture, sedimentary structures, and rock composition. The data was compiled into a vertical stratigraphic column and grouped into lithofacies based on the Ghibaudo (1992) codification. The interpretation stage included determining facies associations based on five parameters: geometry, lithology, sedimentary structures, fossil content, and paleo-current patterns (Selley, 1985). The facies associations were compared to facies models (Mutti & Ricci Lucchi, 1972; Stow, 1985) to determine the depositional environment and sedimentation mechanisms. The final interpretation focused on sedimentation dynamics, including changes in depositional environment, causes of change, and external factors influencing the sedimentation mechanisms.

RESULTS AND DISCUSSION

Stratigraphic Measurement Transect

Stratigraphic data were collected along a measurement transect at the Tonjong River located within the study area. The measured stratigraphic section began at the boundary between the Jampang Formation and the Cikarang Member of the Jampang Formation, situated at UTM coordinates 49 S 432888 E 9141960 N (Figures 3 and 4). Data collection was carried out in a northwesterly direction for 375 meters from the starting point. The stratigraphic measurement along the study transects resulted in a vertical sequence with a total thickness of 86 meters (Figure 5).

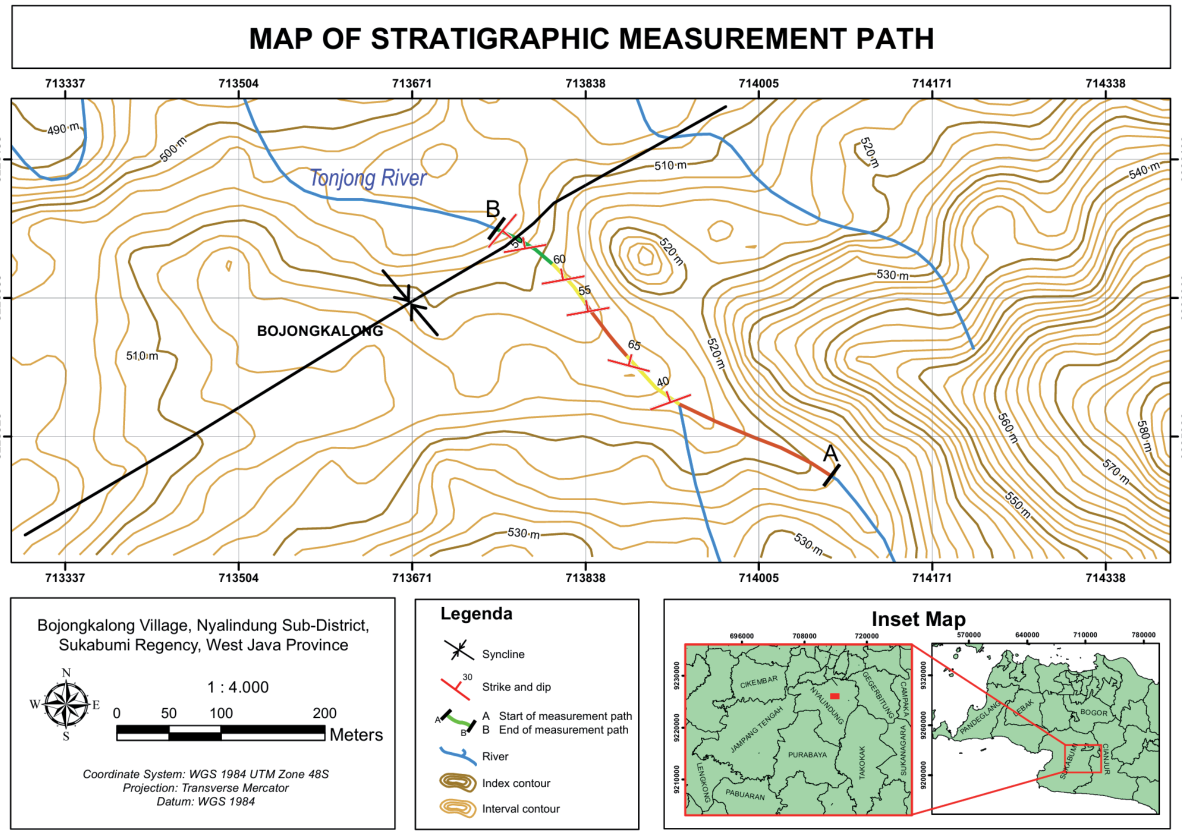

Figure 3. Map of stratigraphic measurement transect.

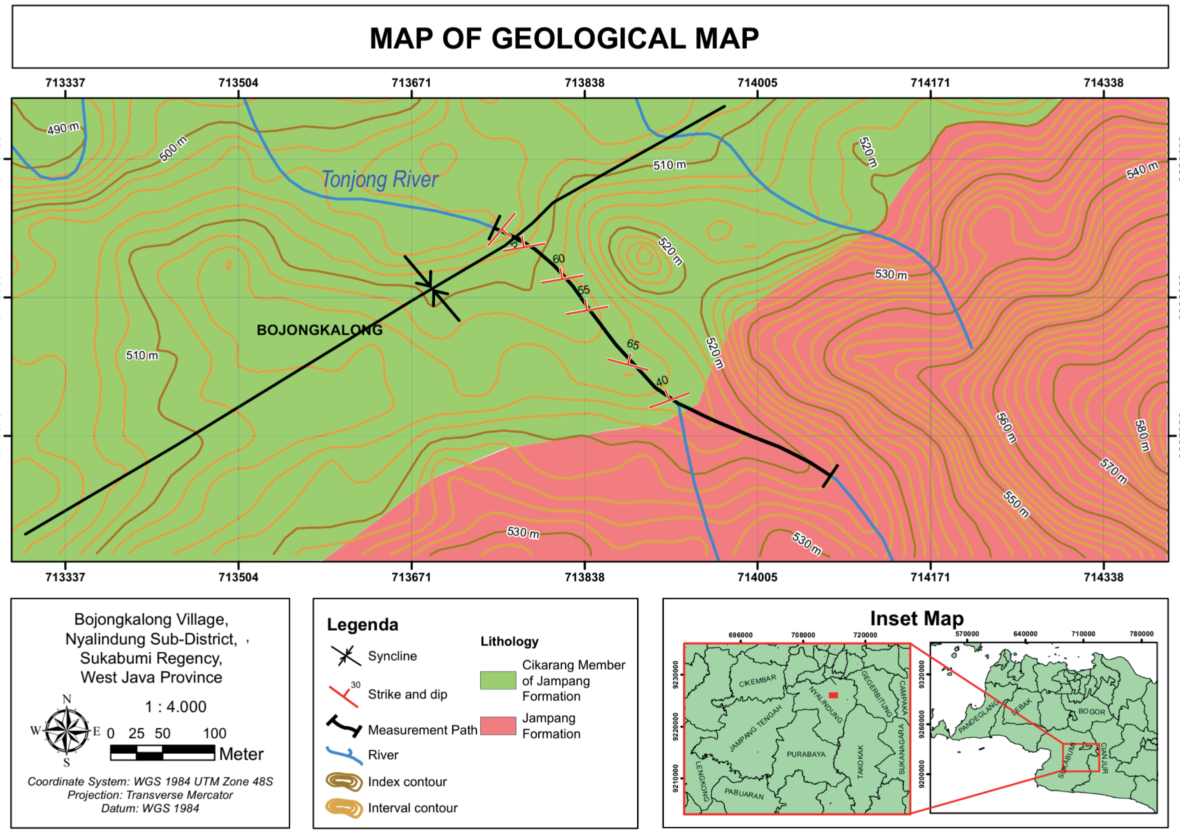

Figure 4. Geological map of study area.

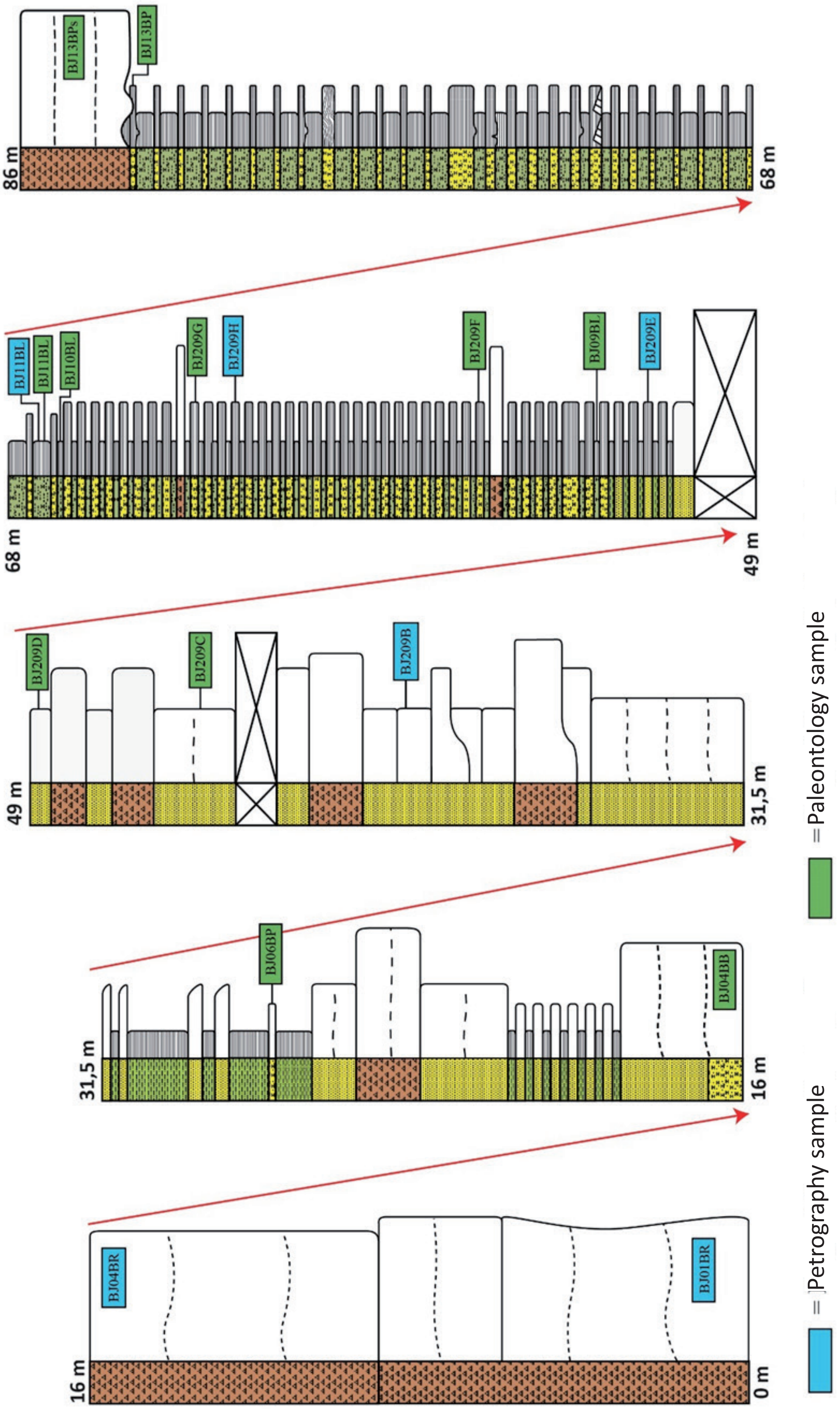

Figure 5. Lithologic column of stratigraphic measurement results.

	Litofasies										
Deskripsi	**Fasies g1G**	**Fasies m1G**	**Fasies mGyS**	**Fasies slSM**	**Fasies mGS**	**Fasies slgMS**	**Fasies mS**	**Fasies sGS**	**Fasies sleSM**	**Fasies sleMS**	**Fasies Fasies sdG**
Ketebalan	6 meter	10 meter, 0.3 meter, 0.3 meter	3 meter	2.8 meter dan 2.1 meter	4.7 meter, 2.1 meter, 5 meter	5.1 meter	3.7 meter	5.6 meter	14.4 meter	16.3 meter	2.7 meter
Posisi	0 - 6 meter	6 - 16 meter, 56.2 - 56.5 meter, 63.9 - 64.2 meter	16 - 19 meter	19 - 21.8 meter dan 50.5 - 52.6 meter	21.8 - 26.5 meter, 40.9 - 43 meter, 44 - 49 meter	26.5 - 31.6 meter	31.6 - 35.3 meter	35.3 - 40.9 meter	52.6 - 67 meter	67 - 83.3 meter	83.3 - 86 meter
Geometri	Batas antar lapisan yang teramalgamasi, menunjukkan kenampakan yang tererosi kuat dan tidak beraturan secara geometri.	Batas antar lapisan yang teramalgamasi, menunjukkan kenampakan yang tererosi kuat dan tidak beraturan secara geometri.	Batas antar lapisan yang teramalgamasi, menunjukkan kenampakan yang tererosi kuat dan tidak beraturan secara geometri.	Singkapan fasies ini menunjukkan rasio ketebalan dari batupasir yang lebih besar dibandingkan batulanau	Batas antar lapisan yang teramalgamasi, menunjukkan kenampakan yang tererosi kuat dan tidak beraturan secara geometri.	Perlapisan ditunjukkan oleh batas tegas dan tidak teramalgamasi dengan rata-rata ketebalan lapisan 7-10 cm	Batas antar lapisan yang teramalgamasi, menunjukkan kenampakan yang tererosi kuat dan tidak beraturan secara geometri.	Batupasir meiliki lapisan yang tebal pada bagian tengah dan menipis menuju arah lateral akibat adanya gerusan oleh batuan yang lebih kasar berupa batupasir kerakalan dan breksi andesit	Ketebalan lapisan batupasir lebih besar dibandingkan batulanau.	Singkapan lapangan menunjukkan rasio ketebalan batulanau karbonatan lebih besar dibandingkan batupasir karbonatan.	Breksi batulanau tersebar secara lateral dengan batas antar lapisan yang teramalgamasi, menunjukkan kenampakan yang tererosi kuat dan tidak beraturan secara geometri
Litologi	Breksi andesit gradasi normal	Breksi andesit masif	Batupasir kerakalan masif	Perselingan batupasir dan batulanau laminasi	Batupasir masif dan Breksi andesit masif	Perselingan batulanau karbonatan dan batupasir karbonatan	Batupasir masif	Perlapisan Batupasir dan Breksi Andesit	Perselingan Batupasir karbonatan dan Batulanau karbonatan	Perselingan Batulanau karbonatan dan Batupasir karbonatan	Breksi batulanau karbonatan hasil mekanisme slide dan slump
Ukuran matriks	Pasir kasar	Pasir kasar	Pasir Kasar	Lanau - Pasir halus	Pasir kasar	Lanau - Pasir Kasar	Pasir sedang - Pasir kasar	Pasir kasar	Lanau - Pasir sedang	Lanau - Pasir sedang	Lanau - Pasir sedang
Ukuran fragmen	Kerikil - Bongkah	Kerikil - Bongkah	Pasir kasar - Kerakal	-	Bongkah	-	Pasir Sangat kasar	Kerakal - Berangkal	-	-	Lanau - Pasir sedang
Sortasi	Buruk, matrix-supported	Buruk, matrix-supported	Buruk, Matrix-Supported	Baik	Baik - Buruk, Matrix-Supported	Baik	Buruk, Matrix-Supported	Buruk, Matrix-Supported	Baik	Baik	Buruk, matrix-supported
Bentuk butir	Subangular-subrounded	Subangular-subrounded	Subangular-Subrounded	-	Subangular-Subrounded	-	Subangular-Subrounded	Subangular-Subrounded	-	-	-
Struktur sedimen	Gradasi normal	Masif	Masif	Perlapisan, rip-up clasts, laminasi	Masif	Gradasi normal, perlapisan, laminasi	Masif	Perlapisan, scour marks, rip-up clasts	Laminasi, perlapisan, load casts dan rip-up clasts, sand dike.	Laminasi, perlapisan, load cast, flame structure, convolute lamination. ripple cross lamination dan rip-up clasts	Masif
Komposisi petrografi	Matriks breksi andesit (BJ01BR) : plagioklas (20%), kuarsa (10%), klinopiroksen (10%), hornblend (5%), litik (30%), mineral opak (5%) dengan matriks mineral kriptokristalin (10%)	Matriks breksi andesit (BJ04BR) : plagioklas (20%), kuarsa (20%), klinopiroksen (10%), ortopiroksen (10%), litik (30%) dengan matriks mineral kriptokristalin (10%)	-	Batupasir (BJ209E) : plagioklas (25%), kuarsa (20%), litik (15%), mineral opak (5%), mineral lempung (15%) dengan matriks mineral kriptokristalin (20%)	-	-	-	Fragmen Breksi (BJ209A) :plagioklas (40%), klinopiroksen (20%), ortopiroksen (15%), mineral opak (5%) dengan matriks mineral kriptokristalin (20%)	Batupasir karbonatan (BJ209H) : plagioklas (20%), kuarsa (15%), mikrofosil (5%), glaukonit (5%), kalsit (10%), litik (10%), mineral opak (10%) dengan matriks mineral kriptokristalin (25%)	Batulanau karbonatan (BJ11BL)komposisi skeletal grain berupa mikrofosil (30%), kuarsa (5%), plagioklas (5%), lempung (15%), dan mineral opak (5%) dengan matriks mineral kriptokristalin kalsit (40%)	-
Nama Petrografi	Lithic arenite (Pettijohn, 1987)	Lithic arenite (Pettijohn, 1987)	-	feldspatic wacke (Pettijohn, 1987)	-	-	-	Andesite (Streckeisen, 1976)	Feldspathic wacke (Pettijohn, 1976)	Muddy micrite (Mount, 1985)	-
Keterdapatan fosil indeks	-	-	-	-	BJ209C dan BJ209D : Dentalina subsoluta, Praeorbulina sicana, Planulina ariminensis, Cibicidoides robertsonianus, dan Bulimina pupoides	BJ06BP : Catapsydrax stainforthi, Amphistegina gibbosa	-	-	BJ09BL, BJ209F, BJ209G, BJ10BL : Globigerinoides diminutus, Bulimina pupoides, Cibicidoides robertsonianus, Fissurina seguenziana, Cibicidoides robertsonianus, Praeorbulina glomerosa	BJ11BL & BJ13BP : Praeorbulina glomerosa, Dentalina subsoluta, Rectoglandulina torrida, Fissurina seguenziana, Fissurina lagenoides, Trilobatus bisphericus, Rectoglandulina comatula	BJ13BPs : Praeorbulina glomerosa dan Globorotaloides suteri
Mekanisme pengendapan	Mekanisme pengendapan cepat dengan transportasi suspensi dan bed-load antar butir melalui aliran konsentrasi tinggi dan dipengaruhi oleh mekanisme "freezing" disebut mekanisme mudflows atau cohesive debris flows	Proses sedimentasi cepat secara en masse yakni terendapkan bersama pada suatu waktu yang sama dengan mekanisme mudflows atau cohesive debris flows	Mekanisme pengendapan cepat en masse oleh frictional freezing dari suatu dispersi sedimen pasir berkonsentrasi tinggi. Terbentuk melalui mekanisme mudflows atau cohesive debris flows dengan aliran turbulen	Mekanisme transportasi arus turbid dengan konsentrasi rendah. Partikel berukuran lanau hingga pasir tertransportasi secara suspensi oleh arus turbulen.	Mekanisme arus turbid dalam konsentrasi tinggi melalui proses pengendapan cepat. Proses transportasi suspensi dan traksi membawa sedimen berukuran pasir dan gravel. Kenampakan masif terendapkan melalui en masse secara cepat oleh adanya frictional freezing	mekanisme pengendapan oleh arus turbid dengan konsentrasi. Pengendapan cepat oleh material pasir yang tersuspensi dalam fluktuasi fluida menghasilkan struktur sedimen gradasi normal pada batupasir.	Mekanisme mudflows atau dapat disebut cohesive debris flows. Hal tersebut ditunjukkan oleh karakteristik batupasir yang sortasi buruk dan matrix supported dengan fragmen kerikilan mengambang pada matriks batupasir kasar.	Pengendapan secara cepat en masse menghasilkan pemilahan butiran yang buruk. penggerusan dari sedimen yang lebih kasar terhadap sedimen yang lebih harus yang dipengaruhi oleh sisa aliran turbulen	Mekanisme arus turbid dengan konsentrasi rendah. Partikel sedimen berukuran lempung hingga pasir sedang tersuspensi oleh aliran turbulen.	Mekanisme pada arus turbid dengan konsentrasi rendah. Partikel sedimen berukuran lempung hingga pasir sedang tersuspensi akibat aliran turbulen	Mekanisme pada arus turbid dengan konsentrasi rendah. Pada fase post-sedimentation, ketika batuan belum terlitifikasi secara sempurna terjadi mekanisme slide dan slump, berupa adanya suatu material bergerak menuruni suatu bidang gelincir pada suatu lereng pengendapan.

Figure 6. Lithofacies description of the Cikarang Member.

Lithofacies

Based on the physical characteristics, sedimentary structures, and composition observed in the outcrops, the lithological components of the study location are divided into 11 lithofacies (Figure 6). The lithofacies are named according to the Ghibaudo (1992) facies codification.

1. Graded Gravel (g1G) Facies
2. Massive Gravel (m1G) Facies
3. Massive Gravelly Sand (mGyS) Facies
4. Plane-Stratified Laminated Sand-Mud Couplets (slSM) Facies
5. Massive Gravel-Sand Couplets (mGS) Facies
6. Plane-Stratified Laminated to Graded Mud-Sand Couplets (slgMS) Facies
7. Massive Sand (mS) Facies
8. Plane-Stratified Gravel-Sand Couplets (sGS) Facies
9. Plane-Stratified Laminated Muddy Interval Sand-Mud Couplet (sleSM) Facies
10. Plane-Stratified Laminated Muddy Interval Mud-Sand Couplets (sleMS) Facies
11. Slide and Slump Deposits Gravel (sdG) Facies

Facies Associations & Depositional Environment

Based on the lithological characteristics, the study area can be divided into 11 lithofacies, namely g1G, m1G, mGyS, slSM, mGS, slgMS, mS, sGS, sleSM, sleMS, and sdG. The paleontological analysis indicates that the study area was deposited in a deep-marine environment. The characteristics of lithofacies, such as variations in lithology and the presence of various sedimentary structures, suggest a deep-sea fan environment. The comparison of the study area facies with previous facies models shows the presence of 4 facies associations that represent the depositional environment:

1. Facies Association 1 (FA 1): Channel

   The channel facies association is characterized by lithological units of andesite breccia and massive sandstone. FA 1 consists of facies g1G, m1G, and mGyS in the 0 - 19 meter interval, as well as facies sGS and mGS in the 35.3 - 49 meter interval. The distinctive features are massive, structureless, poorly sorted, and floating fragments (Figure 7).

   This facies association is interpreted to have deposited in a high-energy environment with a mechanism of mudflows/cohesive debris flows in a channel sub-environment. The depositional pattern shows a fining-upward trend in the lower part (0 - 19 meters), followed by a change in lithology from andesite breccia to sandstone, indicating an increase in transport distance. The middle part (35.3 - 49 meters) shows a coarsening-upward sequence with a decrease in the sandstone ratio and an increase in andesite fragments, as well as the presence of scour marks due to erosion (Figure 8).

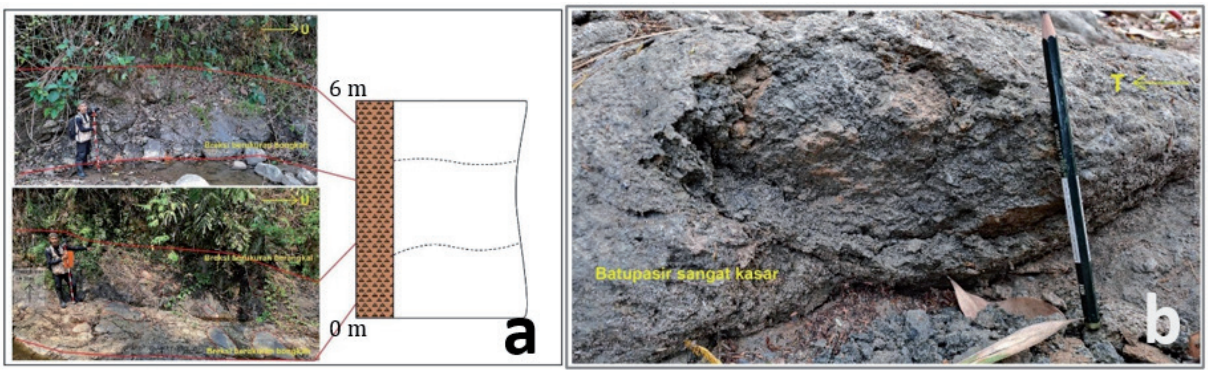

Figure 7. (a) Field observations of the g2G facies reveal an amalgamated andesite breccia with block-sized fragments. (b) The detailed appearance of the mS facies sandstone reveals a very coarse grain size).

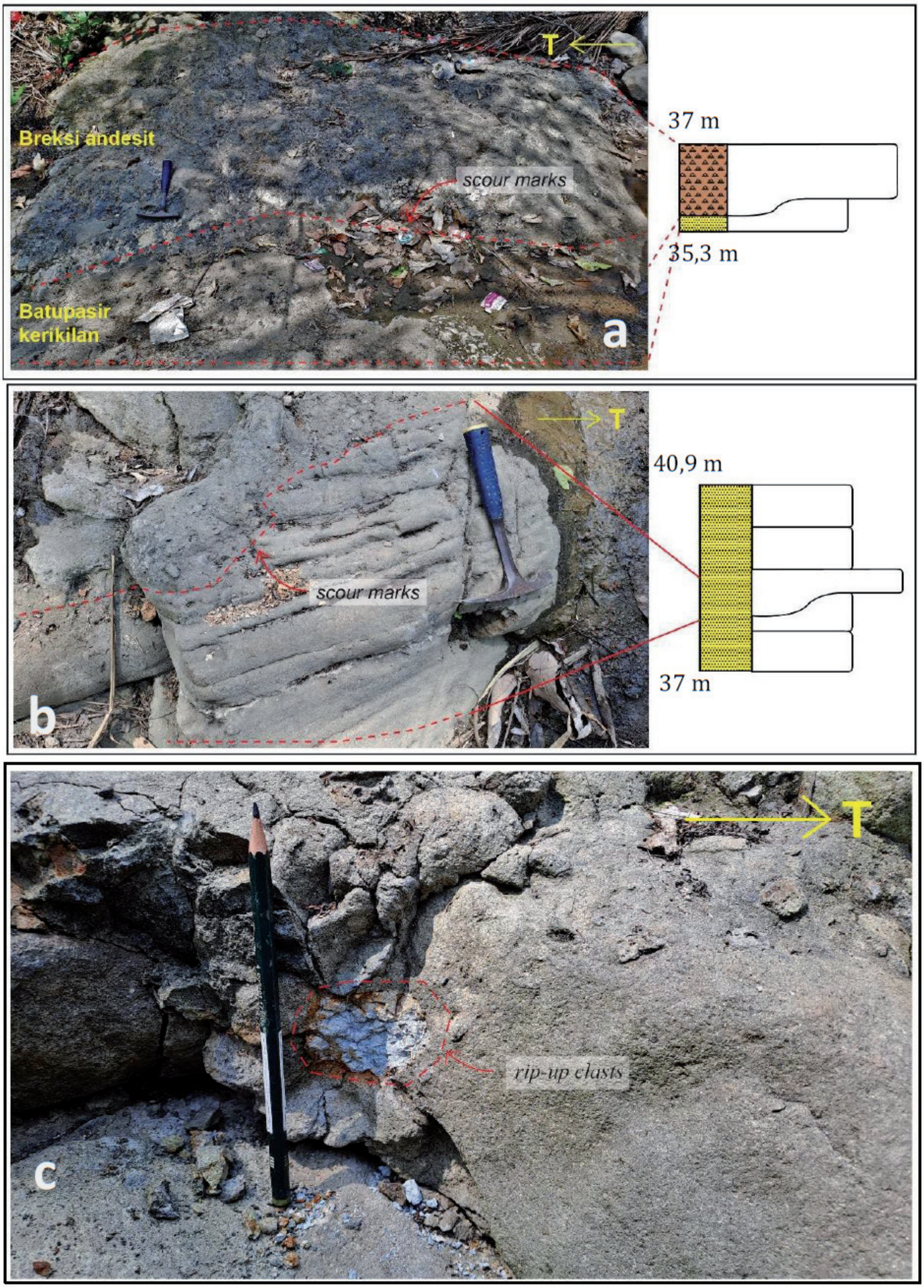

Figure 8. (a) Field observation of scour marks: erosion of coarse sandstone by andesite breccia due to rapid deposition. (b) Field observation of scour marks: erosion of medium sandstone by coarse sandstone due to rapid deposition. (c) Field observation of rip up clasts: whitish-gray sandstone within the sGS facies sandstone.

2. Facies Association 2 (FA 2): Sandy Lobe

FA 2 consists of facies slSM, mGS, slgSM, and mS in the 19-35.3 meter interval, with a total thickness of 16.3 meters (Figure 9). It is composed of interbedded medium-coarse sandstone, siltstone, and andesite breccia, with sedimentary structures such as bedding, lamination, normal grading, sand dikes, and scour marks.

The deposition is interpreted to have occurred in an environment with fluctuating/dynamic energy. The energy pattern begins with low energy (interbedded sandstone-siltstone), then increases (pebbly sandstone-andesite breccia), decreases again (interbedded siltstone-sandstone), and finally increases again (interbedded sandstone-andesite breccia).

There is a change in the depositional mechanism from mudflows (sandstone and breccia) in the lower part to low-density turbidity (interbedded siltstone-normally graded sandstone) in the upper part of the sequence (Figure 10). A distinctive characteristic is the rapid deposition indicated by the sand dike structure due to fluid compression in the siltstone, causing the sandstone to intrude upwards (Figure 11). The overall sequence characteristics show a coarsening-upward succession with an abundance of sandy sediment in the upper part, consistent with the sandy lobe model (Figure 9).

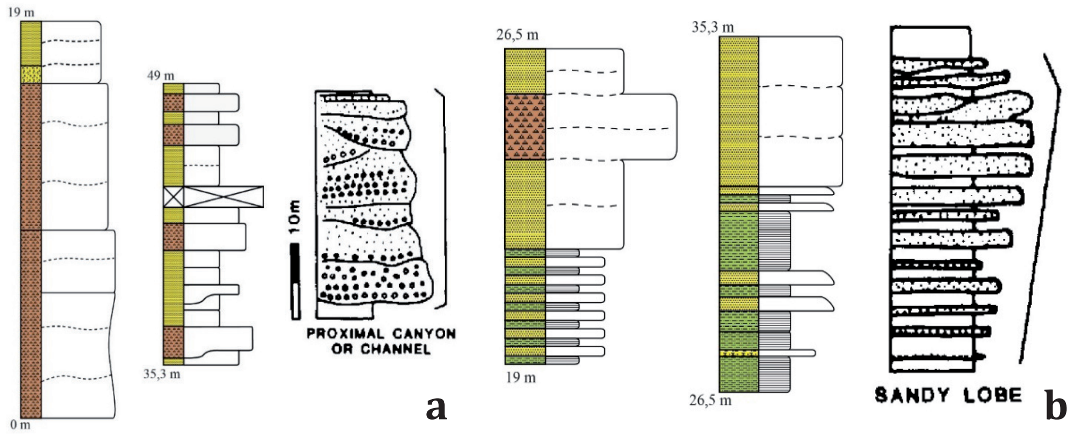

Figure 9. (a) Comparison of Facies Association 1 (FA 1) with the channel facies model (Stow, 1985), (b) Comparison of Facies Association 2 (FA 2) with the sandy lobe facies model (Stow, 1985).

Figure 10. Field observation of slgMS facies shows an alternation of siltstone and sandstone layers, overlain by the mS facies.

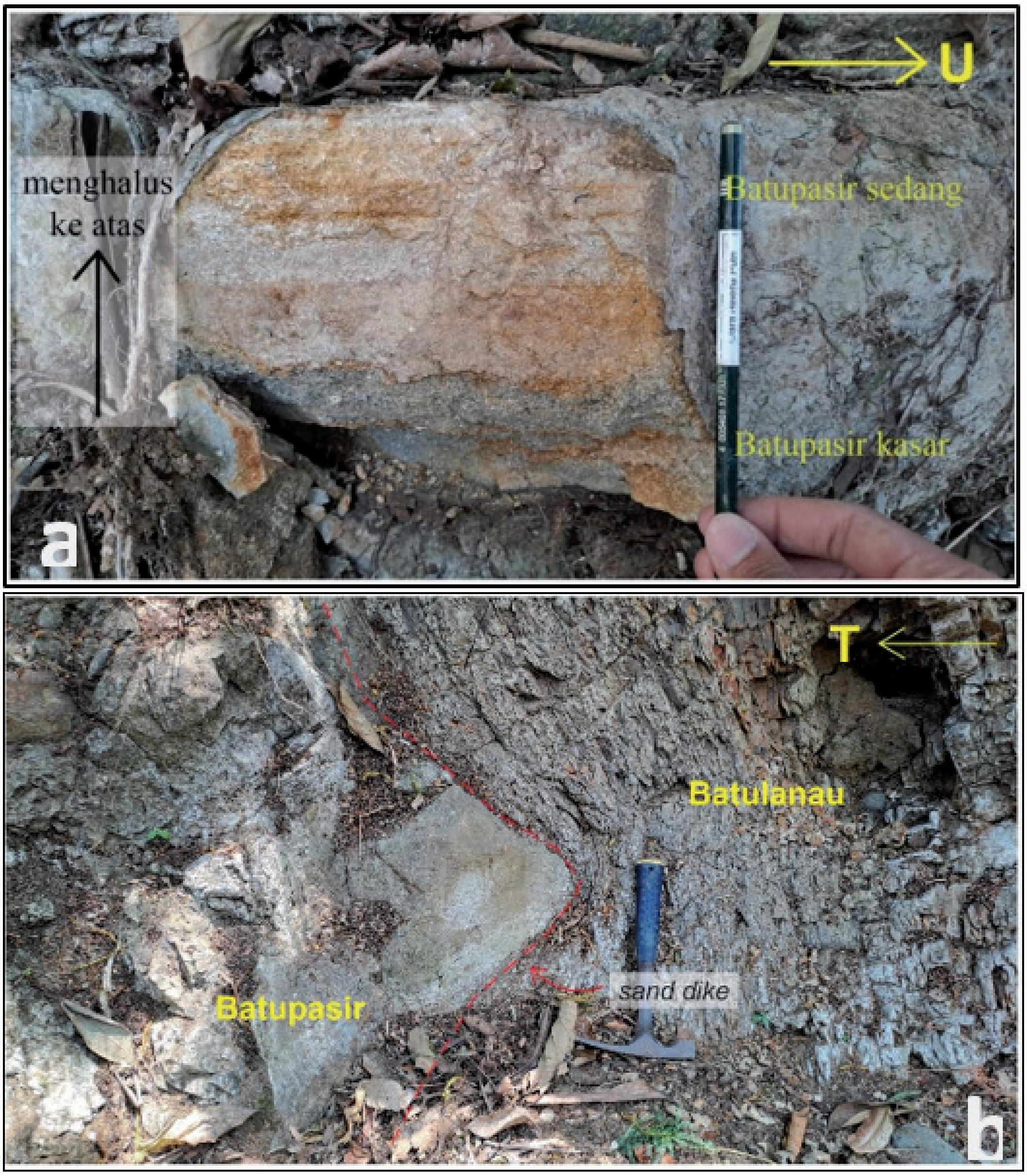

Figure 11. (a) Field observation of normal gradation in slgMS facies sandstone. (b) Field observation of sand dike in slgMS facies sandstone.

3. Facies Association 3 (FA 3): Silty-Sandy Distal Lobes

The Silty-Sandy Distal Lobes Facies Association (FA 3) has a total thickness of 56.6 meters, composed of interbedded medium-coarse sandstone, siltstone, and andesite breccia with sedimentary structures such as bedding, lamination, load casts, and rip-up clasts. The sequence characteristics show a decrease in sandy sediment and an increase in mud/siltstone, without any amalgamated sandstone (Figure 12).

The deposition of FA 3 is interpreted to have occurred in a low-energy depositional environment with a minor increase in energy in the middle part. The dominant mechanism is low-density turbidity. The “freezing” deposition forms the interbedded layers. At the 52.5m interval (Figure 13), carbonate sediment appears. Overall, FA 3 shows a constant succession with a depositional environment distal from the feeder channel. The characteristics of FA 3 include a decrease in depositional energy followed by an increase in fine-grained sediment material.

4. Facies Association 4 (AF 4): Proximal Levee

The Proximal Levee Facies Association (AF 4) is composed of: alternation of calcareous siltstone-calcareous sandstone and andesite breccia. AF 4 has sedimentary structures such as bedding, lamination, rip-up clasts, ripple cross-lamination, load casts, flame structure, and convolute lamination. The mud ratio increases compared to AF 3 (Figure 12). The deposition is interpreted to be the result of turbidity currents and rapid sedimentation, which resulted in load casts (sandstone loading into siltstone), flame structure, and convolute lamination (due to high pore pressure).

Within the AF 4 sequence, a turbidite sequence can be identified, consisting of Ta: medium massive sandstone, Tb: alternating sandstone-siltstone lamination, Tc: sandstone with convolute lamination, Td: laminated siltstone, and the absence of Te, indicating a truncated sequence (Figures 14, 15). The deposition of AF 4 occurred in an environment further from the feeder channel compared to AF 2 and AF 3, as indicated by the finer sediment supply and a drastic decrease in the deposition of coarse particles.

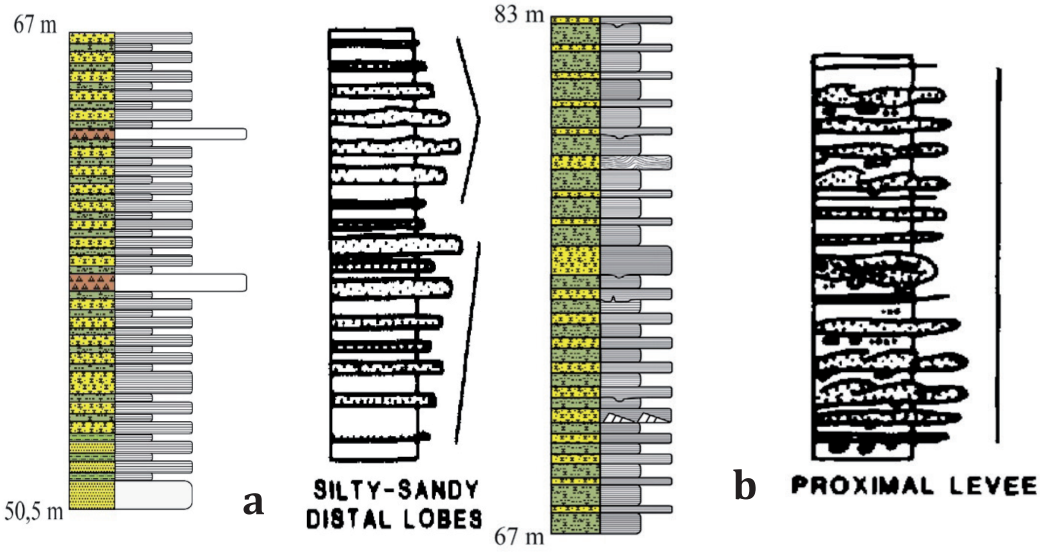

Figure 12. (a) Comparison of Facies Association 3 (FA 3) with the silty-sandy distal lobes facies model (Stow, 1985), (b) Comparison of Facies Association 4 (FA 4) with the proximal levee facies model (Stow, 1985).

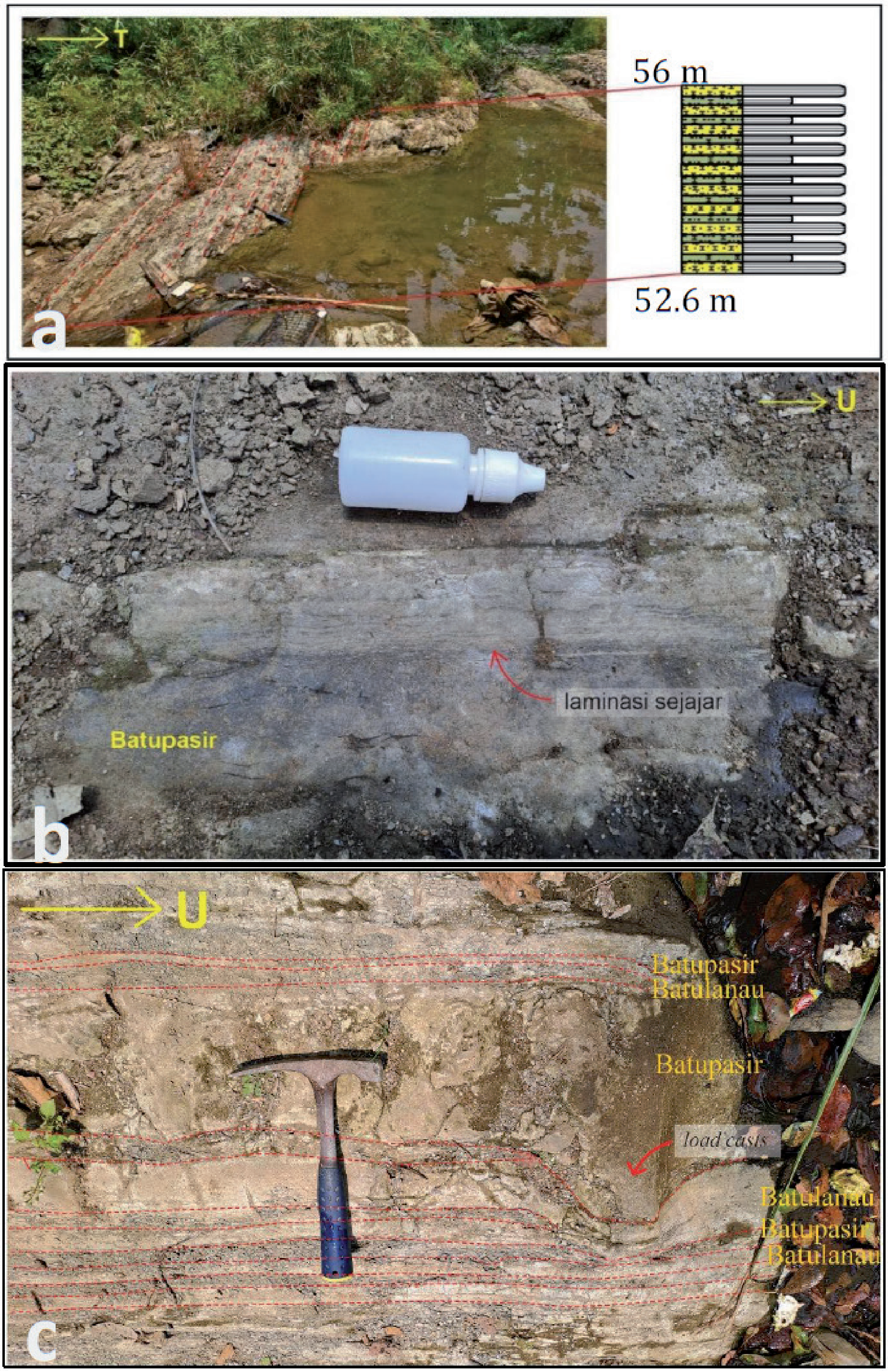

Figure 13. Field observation for FA 3 (a) Field observation of sleSM facies: alternation of calcareous sandstone and calcareous siltstone. (b) Observation of parallel lamination sedimentary structure in calcareous sandstone of sleSM facies. (c) Load casts appearance on sandstone.

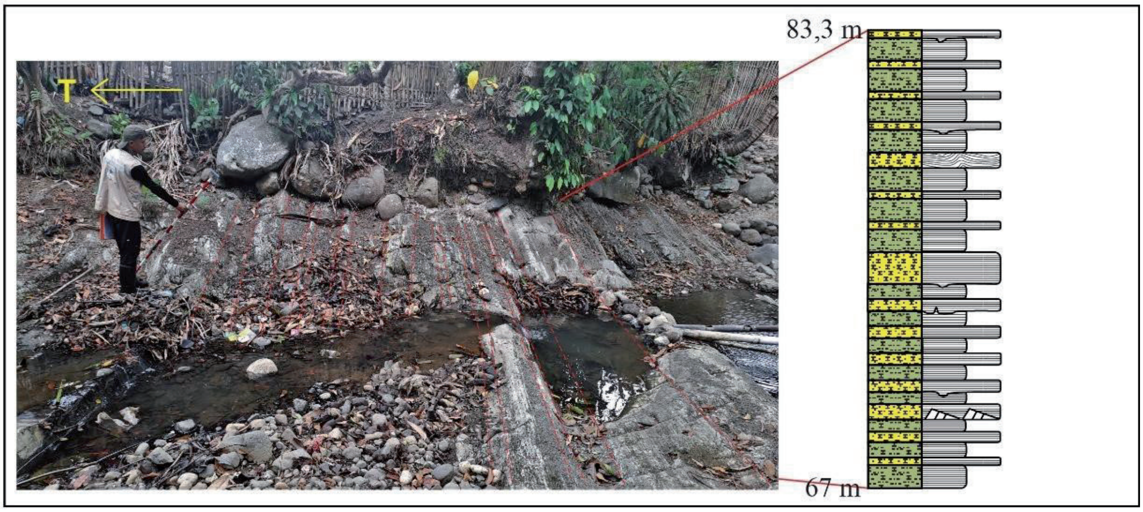

Figure 14. Field observation of sleMS of FA 4 facies shows an alternation of calcareous siltstone and calcareous sandstone.

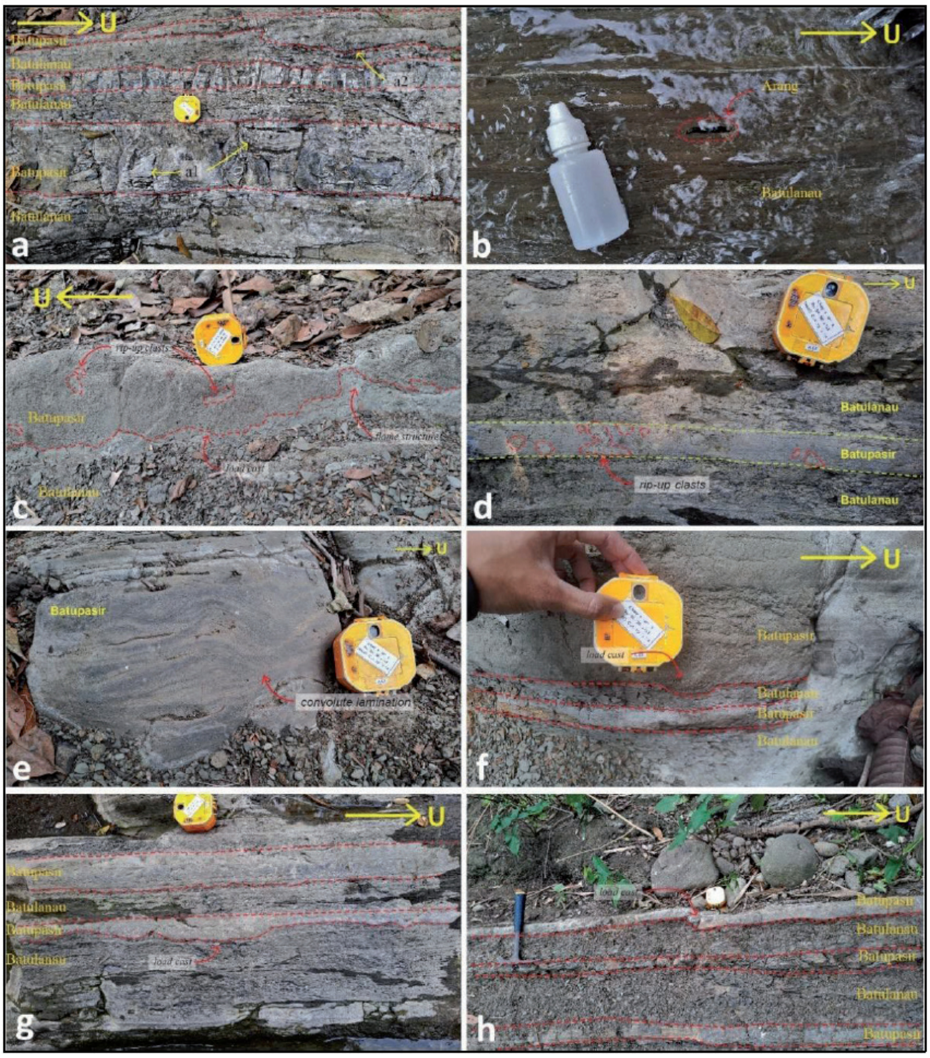

Figure 15. Sedimentary structure observations in sleMS facies of FA 4: (a) Ripple cross lamination (a1) and load cast (a2) on sandstone and siltstone alternation. (b) Rip-up clasts of coal on calcareous siltstone. (c) Flame structure and load cast on siltstone overlain by sandstone. (d) Rip-up clasts of siltstone on sandstone. (e) Convolute lamination on sandstone. (f, g, h) Load casts on sandstone overlying siltstone.

Sedimentation Mechanism

The deposition of the Cikarang Member of the Jampang Formation in the study area began in the Early Miocene, precisely in N7, with the Channel sub-environment (FA 1) (Figures 16, 17). The sequence characteristics indicate deposition by high-energy mudflows, resulting in andesite breccia and pebbly sandstone with constant bathymetry in the middle bathyal. The depositional pattern shows a fining-upward succession.

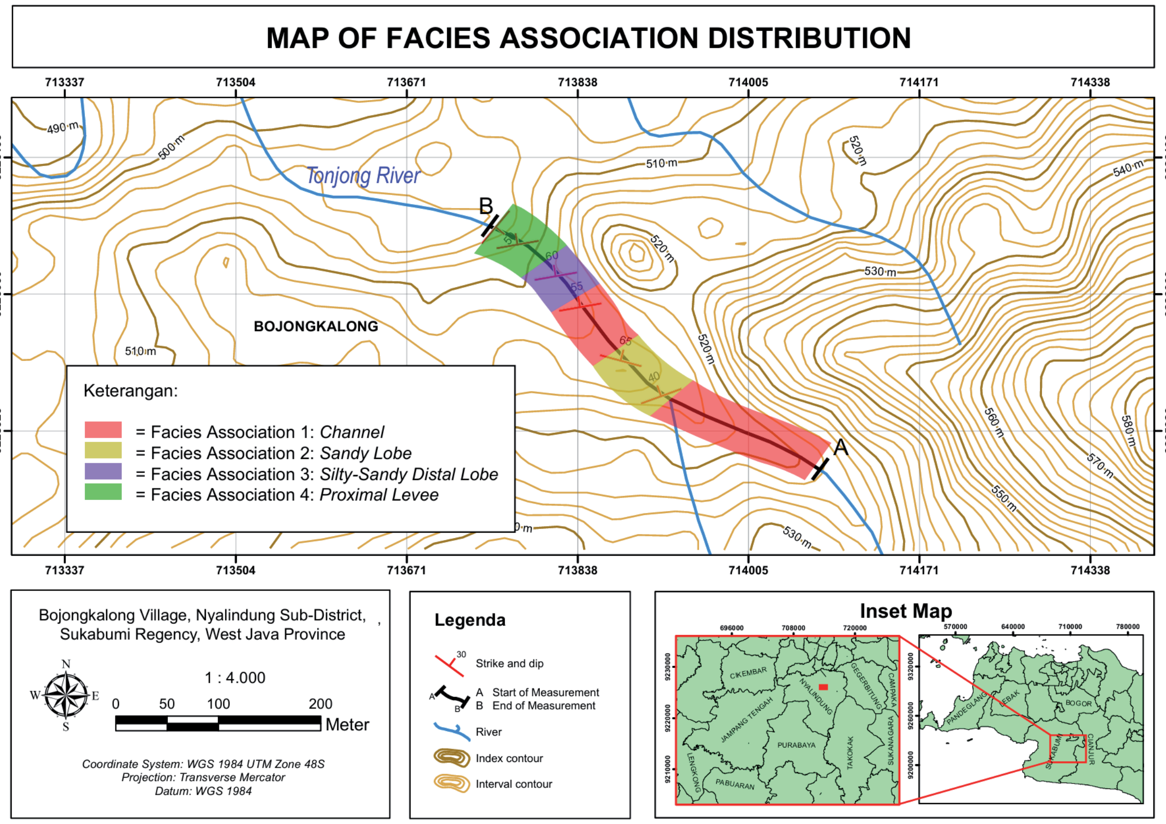

Figure 16. Map of facies association distribution

The next stage was deposited in the Sandy Lobe - Inner Fan sub-environment (FA 2) in the N7 age. The fluctuating depositional energy resulted in the lithology of interbedded sandstone-siltstone and andesite breccia. Changes in bathymetry from middle bathyal to lower bathyal, with sediment supply of andesite breccia fragments originating from the volcanic activity of the Jampang Formation.

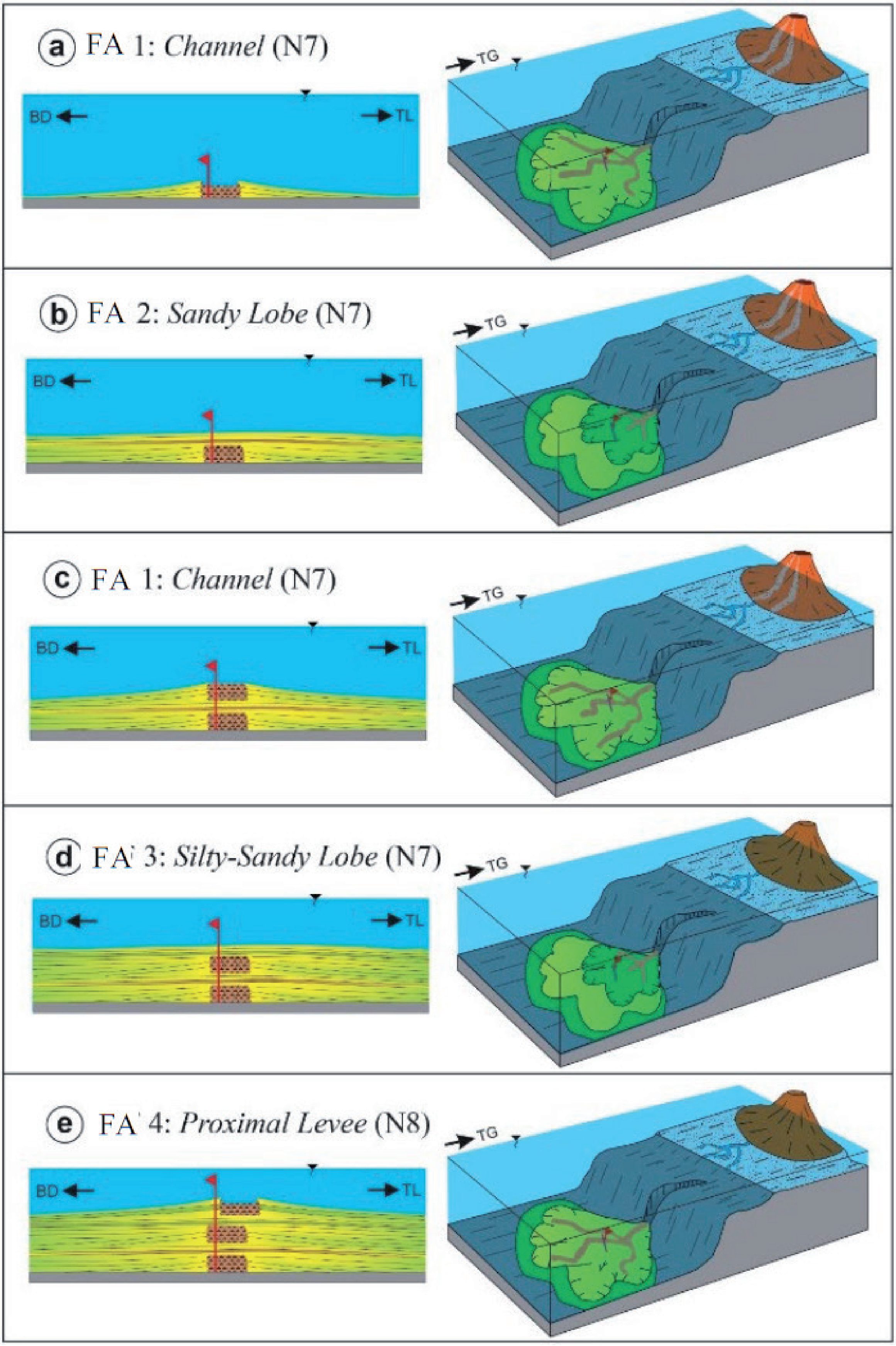

Figure 17. Model of the deposition mechanism for each facies association phase in the form of a three-dimensional (right) and two-dimensional (left) model. Modified after Ma'arif (2015).

The Silty-Sandy Distal Lobes with N7 - Middle Fan (FA 3) age as a depositional sub-environment that is increasingly distant from the feeder channel. The sequence characteristics show a decrease in coarse sediment and an increase in fine sediment deposited through low-density turbidity mechanisms. Carbonate material began to be deposited at a thickness of 52.5 meters. This facies sequence was deposited in a fluctuating bathymetry between middle bathyal and lower bathyal.

The final stage of proximal levee - FA 4 is the final sub-environment with N8 age that is further away from the feeder channel. The deposition mechanism is influenced by low-density turbidity with various sedimentary structures such as load casts, flame structure, convolute lamination, ripple cross-lamination, and rip-up clasts. The bathymetry is in the middle bathyal to lower bathyal. The deposition ends with the sdG facies resulting from the slide and slump mechanism.

Based on the interpretation of the sedimentation mechanism, the vertical sequence of 0 - 16 meters thickness represents sediment material that is characteristic of the Jampang Formation, which is dominated by volcanic influence. While the thickness of 16 - 86 meters correspond to the characteristics of the Cikarang Member, which is an interbedding of sandstone-siltstone with abundant carbonate material.

Previous research refers to the study of the Cikarang Member by Pratiwi et al. (2022) located in the Ciletuh Area. This area is approximately 100 km from the research area. Pratiwi et al. (2022) mentioned that the lithological composition consists of sandstone and claystone, which shares similar characteristics with this study. However, Pratiwi et al. (2022) showed that the lithological composition dates from NN 1 – NN 4, covering the entire Early Miocene period. In contrast, this study indicates that the lithological composition dates from N7 – N8, encompassing the late Early Miocene. This suggests that the lithological composition in the research area represents the uppermost Cikarang Member, which is younger compared to the Cikarang Member in Ciletuh.

CONCLUSIONS

The volcaniclastics of Cikarang Member of Jampang Formation consist 11 facies: graded gravel (g1G), massive gravel (m1G), massive gravelly sand (mGyS), plane-stratified laminated sand-mud couplets (slSM), massive gravel-sand couplets (mGS), plane-stratified laminated to graded mud-sand couplets (slgMS), massive sand (mS), plane-stratified gravel-sand couplets (sGS), plane-stratified laminated muddy interval sand-mud couplets (sleSM), plane-stratified laminated muddy interval mud-sand couplets (sleMS), and slump and slide deposits gravel (sdG). All these facies are deposited in the inner fan – middle fan with a middle bathyal to lower bathyal paleobathymetry in a depositional sub-environment of channel, which then underwent a change to sandy lobes, and was then transformed back into a channel due to sea level fluctuations, followed by a change to silty-sandy distal lobes with sea level rise and fall, and finally changed to a proximal levee with a constant middle bathyal paleobathymetry. The volcaniclastics were deposited through turbidite deposition mechanisms resulting from turbulent flows, with variations of cohesive debris flows (mudflows) and turbidity currents. Mudflows have a depositional pattern that produces Facies Association 1 (FA 1) in the channel sub-environment. Meanwhile, turbidity currents develop in Facies Association 3 (FA 3) and Facies Association 4 (FA 4). In FA 2, it shows variations in the fluctuation of mudflows and low-density turbidity currents.

ACKNOWLEDGEMENTS

All praise and gratitude are bestowed upon Allah SWT, the Almighty God, for His blessings and grace, which have enabled the author to complete this paper. I would like to express my sincere gratitude to Dr.Eng. Ir. Akmaluddin, S.T., M.T., IPM. and Mr. Saptono Budi Samodra, S.T., M.Sc. for providing knowledge, support, critique, suggestions, and guidance during the process of preparing this paper. The author would also like to thank the field team who have assisted in collecting primary data in the field.

REFERENCES

Alif, S. A., 2011, Geologi Sejarah Daerah Sukabumi - Pelabuhan Ratu: Bulletin of Scientific Contribution, v. 9, no. 1, p. 42–48, doi: https://doi.org/10.24198/bsc%20geology.v9i1.8262.g3809

Armandita, C., Mukti, M.M. and Satyana, A.H., 2009. Intra-Arc Trans-Tension Duplex of Majalengka to Banyumas Area: Prolific Petroleum Seeps and Opportunities in West-Central Java Border. Indonesian Petroleum Association Annual Convention and Exhibition, IPA09-G-173.

Barker, R.W., 1960. Taxonomic Notes: Oklahoma, Society of Economic Paleontologist and Mineralogist, 272 p.

Boggs, Jr., S., 2nd eds., 2009, Petrology of Sedimentary Rocks: Cambridge University Press, 600 p.

Bolli, H.M., Saunders, J.B., Perch-Nielsen, K., 1985, Plankton Stratigraphy: Volume 1, Planktic Foraminifera, Calcareous Nannofossils and Calpionellids: Cambridge University Press, 1040 p.

Effendi, A. C., Kusnama, Hermanto, B., 1998, Peta Geologi Lembar Bogor, Jawa: Pusat Penelitian dan Pengembangan Geologi (P3G), skala 1:100.000, 1 lembar.

Etter, W., 2024, A report on palaeontological excavations and sampling in mudrocks: some guidelines: Swiss Journal of Palaeontology, v. 143, 11 p., doi: https://doi.org/10.1186/s13358-024-00305-w

Fitri, D.B., Hidayat, B., dan Subandrio, A.S., 2017, Klasifikasi Jenis Batuan Sedimen Berdasarkan Tekstur Dengan Metode Gray Level Co-occurrence Matrix Dan K-nn, dalam Proceeding, e-Proceeding of Engineering, Volume 4, Nomor 2, Agustus 2017, p. 1638–1645.

Ghibaudo, G., 1992, Subaqueous sediment gravity flow deposits: practical criteria for their field description and classification: Sedimentology, v. 39, p. 423-454, doi: https://doi.org/10.1111/j.1365-3091.1992.tb02126.x.

Haryanti, T., 2006, Stratigrafi dan Sedimentasi Endapan Vulkanik Formasi Nglanggran pada Jalur Kali Putat dan Kali Pentung, Kabupaten Gunung Kidul Daerah Istimewa Yogyakarta, (skripsi tidak dipublikasikan): Yogyakarta, Universitas Gadjah Mada, 83 p.

Hidayat, A.F., Rosana, M.F., Haryanto, A.D., 2021, Geologi Daerah Langkaplancar dan Sekitarnya, Kecamatan Langkaplancar, Kabupaten Pangandaran, Provinsi Jawa Barat: Padjadjaran Geoscience Journal, v. 5, p. 59–70.

Intan, M.F.S., dan Manurung, F., 2022, Geologi Situs Ciomas di Kabupaten Sukabumi: Kajian Sumber Batuan untuk Bahan Litik: Naditira Widya, v. 16, p. 73-84, doi: https://doi.org/10.24832/nw.v16i1.497

Khodijah, S., Pratiwi, S. D., Rosana, M., F., 2023, Geologi Daerah Gunungbatu dan Sekitarnya Kecamatan Ciracap, Kabupaten Sukabumi, Provinsi Jawa Barat: Padjadjaran Geoscience Journal, v. 7, p. 1285–1296.

Lowe, D.R., 1979, Sediment Gravity Flows: Their Classification and Some Problems of Application to Natural Flows and Deposits: Geology of Continental Slopes, v. 27, p. 75–82, doi: https://doi.org/10.2110/pec.79.27.0075

Ma'arif, S.G., 2015, Dinamika Sedimentasi Batuan Formasi Halang di Daerah Kalisalak, Kecamatan Margasari, Kabupaten Tegal, Provinsi Jawa Tengah, (skripsi tidak dipublikasikan): Yogyakarta, Universitas Gadjah Mada, 200 p.

Martodjojo, S., 2003, Evolusi Cekungan Bogor, (disertasi doktor tidak dipublikasikan): Bandung, Institut Teknologi Bandung, 258 p.

McPhie, J., Doyle, M., Allen, R., 1993., Volcanic Textures: a guide to the interpretation of textures in volcanic rocks: Tasmania, University of Tasmania. 211 p.

Mukti, M.M. and Ito, M., 2010. Discovery of outcrop-scale fine-grained sediment waves in the lower Halang Formation, an upper Miocene submarine-fan succession in West Java. Sedimentary Geology, 231(3-4), pp.55-62.

Mukti, M.M., Ito, M. and Armandita, C., 2009. Architectural Elements of a Longitudinal Turbidite System: The Upper Miocene Halang Formation Submarine-Fan System in the Bogor Through, West Jawa. Indonesian Petroleum Association Annual Convention and Exhibition, IPA09-G-168

Muljana, B., 2023, Evolusi Tektonisme dan Magmatisme sebagai Kontrol Cebakan Emas di Cineam, Kabupaten Tasikmalaya, Jawa Barat: Bulletin of Scientific: Geology, v. 21, p. 81–88, doi: https://doi.org/10.24198/bsc%20geology.v21i2.48495.

Mutti, E., dan Ricci Lucchi, F., 1972, Le torbiditi dell'Appennino Settentrionale: introduzione all'analisi di facies: Memorie Della Società Geologica Italiana, v. 11, p. 161199.

Nova F., M.Z., Abdurrokhim, Firmansyah, Y., 2018., Studi Litofasies dan Lingkungan Pengendapan Formasi Halang pada Lintasan Sungai Ciwaru, Majalengka, Jawa Barat: Padjadjaran Geoscience Journal, v. 2, p. 96–102.

Novita, D., Sanjaya, I., Margono, U., Mawardi, S., 2016., Peta Geologi Inderaan Jauh Lembar Sukabumi (1209-12) Jawa: Pusat Survei Geologi, Badan Geologi, Kementrian Energi dan Sumber Daya Mineral, skala 1:50.000, 1 lembar.

Postuma, J.A., 1971, Manual of planktonic Foraminifera: Amsterdam, Elsevier, 420 p.

Pratiwi, S.D., Chiyonobu, S., & Rosana, M.F., 2022, Identifikasi Umur Formasi Jampang Anggota Cikarang Berdasarkan Kumpulan Nannofosil Gampingan di Sungai Cikarang, Geopark Ciletuh Pelabuhan Ratu: Bulletin of Scientific Contribution: Geology, v. 20, p. 137–142, doi: https://doi.org/10.24198/bsc%20geology.v20i3.44145.g19291

Pusat Survei Geologi, 2016, Kolom Stratigrafi Rinci Survei Pemetaan Geologi lembar Sukabumi skala 1:50.000. Laporan Pusat Survei Geologi, Bandung (Tidak diterbitkan).

Schmid, R., 1981, Descriptive nomenclature and classification of pyroclastic deposits and fragments: Recommendations of the IUGS Subcommission on the Systematics of Igneous Rocks: Geologische Rundschau, v. 70, p. 794–799, doi: https://doi.org/10.1007/BF01822152

Selley, R.C., 3rd eds., 1985, Ancient sedimentary environments and their subsurface diagnosis: Springer-Science & Business Media, B.V., 332 p.

Shanmugam, G., 1997, The Bouma Sequence and the turbidite mind set: Earth-Science Reviews, v. 42, p. 201–229, doi:10.1016/S0012-8252(97)81858-2.

Stow, D.A.V., 1985. Deep-sea clastics: where are we and where are we going? Geological Society, London, Special Publications, 18(1), pp.67-93.

Sukamto, R., 1975, Peta Geologi Lembar Jampang dan Balekambang Jawa Barat: Pusat Penelitian dan Pengembangan Geologi (P3G), skala 1:100.000, 1 lembar.

Verdiana, P. R. M., Yuniardi, Y., Nur, A. A., 2014, Petrologi dan Petrografi Satuan Breksi Vulkanik dan Satuan Tuf Kasar pada Formasi Jampang, Daerah Cimanggu dan Sekitarnya, Jawa Barat: Bulletin of Scientific Contribution: Geology, v. 12, p. 171–179, doi: https://doi.org/10.24198/bsc%20geology.v12i3.8378

Walker, R.G., dan James, N.P., 1992, Facies models: Response to Sea Level Change: Geological Association of Canada, 407 p.